

Mass transportation of thermally driven nanotube nanomotors with defects

Jige Chen^{1,*}, Yi Gao¹, Chunlei Wang¹, Renliang Zhang¹, Hong Zhao², and Haiping Fang¹
¹Shanghai Institute of Applied Physics, Chinese Academy of Sciences, Shanghai 201800, China and
²Department of Physics, Xiamen University, Xiamen 361005, China

Thermally driven nanotube nanomotors provide linear mass transportation controlled by a temperature gradient. However, the underlying mechanism is still unclear where the mass transportation velocity in experiment is much lower than that resulting from simulations. Considering that defects are common in fabricated nanotubes, we use molecular dynamics simulations to show that the mass transportation would be considerably impeded by the potential barriers or wells induced by the defects, which provides a possible picture to understand the relative low value at microscopic level. The optimal structure and the factors which would affect the performance are discussed. The result indicates considering defects is helpful in designing nanotube nanomotor and other new nanomotor-based devices.

PACS numbers: 65.80.-g, 81.07.Nb, 85.35.Kt, 65.40.De

INTRODUCTION

Controlled mass transportation is the key function of the molecular motor. Nature already provides some biological nanomotors, which however can only work in specific environmental conditions[01–03]. In contrast, nanotube nanomotors[04, 05] can operate in diverse environments that include various chemical media, as well as electric or magnetic fields[06–12]. Their multiple advantages make them capably evolved into components of versatile nanodevices in applications. Pressure gradients, mechanical force, and electrical bias, et al. are the possible driving forces[04, 05, 13, 14] in nanotube nanomotors. Recently, the use of thermal gradient to actuate mass transportation have been demonstrated to be highly valuable in nanotube nanomotor design[08–12]. Thermophoresis, also known as the Soret effect, is capable of driving fluids, gases, DNA molecules and other nano materials that are subjected to a thermal gradient. In 2008, the first successful fabrication of a thermally driven nanotube nanomotor was reported by Barreiro et al[09]., in which the outer tube of a double-walled carbon nanotube (DWNT) traveled along a coaxial inner tube by actuation of a temperature gradient. Later, mass transportation of carbon nanotube (CNT) capsules, the inner tube of a DWNT, graphene nanoribbons and other nano materials were experimentally realized or theoretically proposed[08, 10, 11, 15–21].

Although the underlying mechanism of thermophoresis is still unclear, there is a growing interest in the scientific community to design and fabricate thermally driven nanotube nanomotor due to its practical usability and potential applications. We note that in most simulations, the average mass transportation velocity is about 1-2 Å/ps ($1-2 \times 10^8$ um/s), while it is only 1-2 um/s in experiments—this is 7 orders of magnitude lower than the simulation value. Besides the small system dimension and large temperature gradient limited by the calculation capabilities[09], no other picture is provided to understand origin of the stagnation at microscopic level. Meanwhile, defects are common in practically fabricated nanotubes according to results from scanning tunneling microscope observations as well as quantum and classical

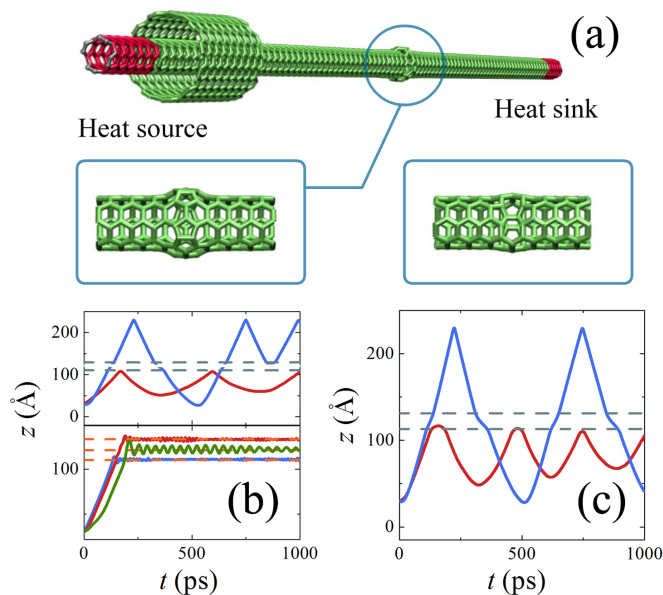


Figure 1: System and kinetic results. (a) Schematic of the nanotube nanomotor. The fixed atoms are silver, and the atoms at the heat source and heat sink are red. The carbon ad-dimer (CD) defects (left) or Stone-Wales (SW) defects (right) are placed in the middle of the inner tube. (b, c) The axial trajectory z of the center of mass (COM) of the outer tube as a function of simulation time, t , along the inner tube, with (b) CD defects and (c) SW defects, as determined by independent simulations. The dashed lines indicate the possible bouncing or trapping sites.

simulations[22–28]. The properties of CNTs would be drastically modified in the presence of those defects. The most common defects, such as carbon ad-dimer (CD) defects[23–25] and Stone-Wales (SW) defects[26–28], are usually induced by one or more pentagon-heptagon (5-7) pairs in CNTs. They produce changes in the topological structure and consequently affect the electronic, mechanical, and thermal properties of CNTs. Despite the significant impact and inevitable presence of defects, their explicit effect upon the mass transportation of nanotube nanomotors has not been reported.

In this paper, we use molecular dynamics (MD) simulations

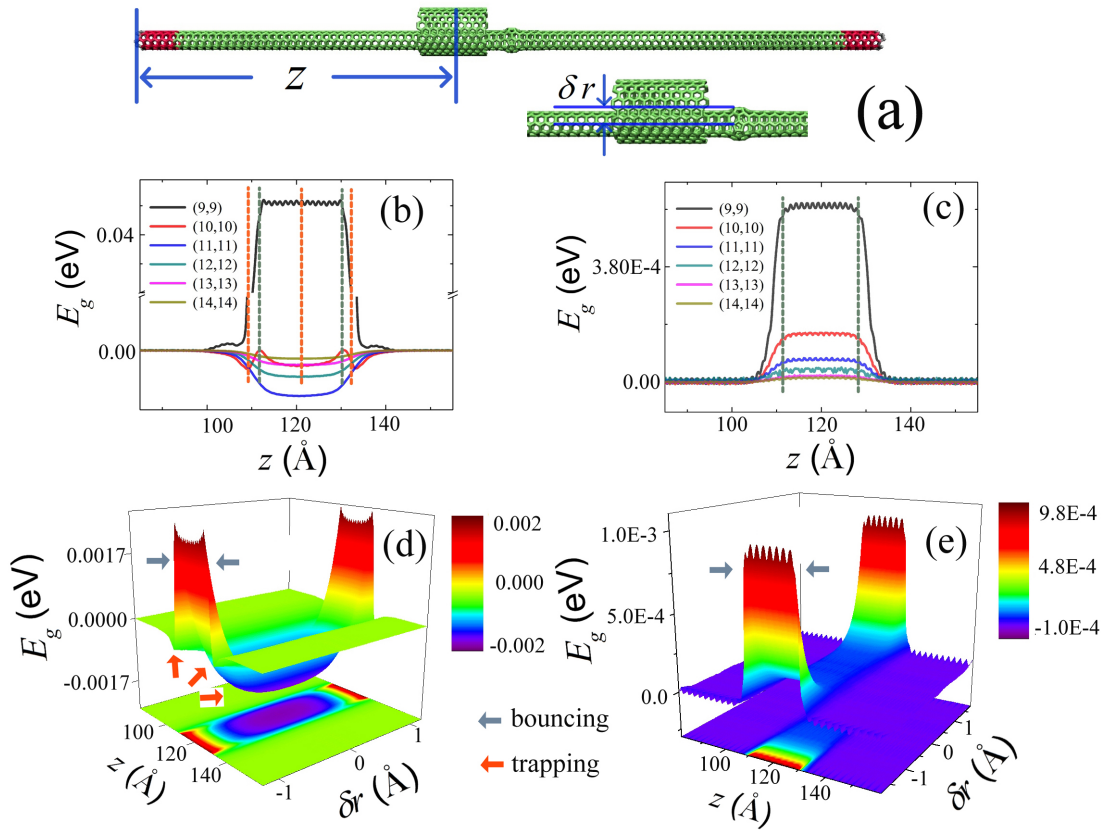


Figure 2: Van de Waals energy change E_g induced by defects. (a) Schematics of the axial coordinate and the deviation distance δr . (b, c) E_g as a function of z around the (b) CD defects and (c) SW defects. The chirality vector of the outer tube ranges from (9, 9) to (14, 14). The possible bouncing (trapping) sites are indicated by dashed cyan (orange) lines. (d, e) E_g as a function of both z and δr around the (d) CD defects and (e) SW defects in the (4, 4)/(11, 11) DWNT. The possible bouncing and trapping sites are indicated by arrows.

to investigate defective nanotube nanomotor and find out the mass transportation might be considerably impeded by defects, which gives a possible picture to understand the relatively low transportation velocity.

METHODS

The nanotube nanomotor consists of a 24 nm long (4, 4) inner tube and a 2 nm long outer tube with chirality vector ranging from (9, 9) to (14, 14). Two most common defects, namely, the carbon ad-dimer (CD) and the Stone-Wales (SW) defects, are placed in the middle of the inner tube. The CD defect is a 7-5-5-7 defect formed by adsorption of a carbon dimer[23–25]. The SW defect is a 5-7-7-5 defect formed by the $\pi/2$ rotation of a C-C bond[26–28]. Their initial geometries are determined using a topological defects generating algorithm based on the MM3 Allinger force field[29, 30]. Figure 1(a) shows the initial structure of the DWNT. An MD package LAMMPS[31] and the AIREBO potential[32] are used to perform the MD calculations. A minimum time step of 1 fs is employed for all of the simulations.

The simulations are performed in three steps:

- (1) The first step consists of isothermal equilibration in which the DWNT is thermalized at 300 K for 100 ps.
- (2) The second step consists of the non-equilibrium MD simulation. Two slabs, one at each end of the inner tube, are used as the heat source and heat sink. The temperature gradient is established by implementing a constant heat flux (4 eV/ps) for 1 ns[33].
- (3) The third step consists of the mass transportation of the outer tube. At this stage, the restriction on the outer tube is removed. It is the actual production run for 1 ns.

RESULTS AND DISCUSSION

Figure 1 shows the typical axial trajectories of the center of mass (COM) of the outer tube. When encountering CD defects, the outer tube may exhibit three phenomena: (1) It passes through the defects, (2) It bounces back, and (3) It is trapped at some specific sites. Similarly, upon encountering the SW defects, the outer tube exhibits (1) and (2) phenomena. The dash lines in Fig. 1 represent the possible bouncing and trapping sites. Furthermore, the outer tube is still possible to pass through the defects after bouncing back or trapping for a

long time.

To understand the microscopic mechanism of the impedance, we analyze the change of van de Waals energy induced by the defects as:

$$E_g = \frac{\sum_{i=1}^N V'_i - V_i}{N} \quad (1)$$

where V'_i (V_i) is the van de Waals energy between the i th atom in the outer tube and the other atoms in the DWNT with defective (perfect) inner tube, and N is the total number of atoms in the outer tube. Therefore E_g describes the average change of van de Waals energy when the outer tube encounters the defects. E_g varies according to the configuration between the inner and the outer tubes. For simplicity, we only consider three factors: (1) Axial coordinate z of the COM of the outer tube, (2) Deviation distance δr between the two tubes in Fig. 2(a), (3) Deviation angle $\delta\alpha$ between the two tubes in Fig. 4. Since $\delta\alpha$ is small during the mass transportation process (see Fig. 4(d) later), its contribution is usually neglected. We first investigate the van de Waals energy change induced by the CD defects. Fig. 2(b) shows E_g varying as a function of z , and Fig. 2(d) shows E_g varying as the function of both z and δr . It shows that the possible bouncing sites correspond to the edges of the potential barriers, and the possible trapping sites correspond to the bottoms of potential wells. Similar E_g distributions are observed around the SW defects in Fig. 2(c) and (e).

The above observations indicate that at microscopic level, defects ruins the perfect crystal structure and remarkably impede the mass transportation of the nanotube nanomotor. It leads to a possible relationship between the low transportation velocity and surface roughness at macroscopic level. The characteristic of the defects are represented by the van de Waals energy change E_g , rather than the absolute potential energy V_i or V'_i . As shown in Fig. 2, the defects are quite small comparing with either the inner or outer tube. Once away from the defects, E_g drops to approximately zero quickly. The kinetic behavior change (bouncing and trapping) also occurs near the defects. Therefore, in the large fabricated DWNT system for applications (with either larger diameter or tube length) or considering other nanotube system with different potential parameters, although the potential energy V_i or V'_i may differ from present simulations, similar van de Waals energy change E_g would lead to similar kinetic behaviors.

We attempted to determine the optimal structure to minimize the stagnation. Therefore we define a passing ratio to measure the robustness of the nanotube nanomotor as:

$$\eta_{\text{passing}} = \frac{N_{\text{passing}}}{N_{\text{passing}} + N_{\text{bouncing}} + N_{\text{trapping}}} \quad (2)$$

where N_{passing} , N_{bouncing} , and N_{trapping} are the numbers of times that the outer tube passes through the defects in less than 30 ps, bounces back, and is trapped respectively. We also

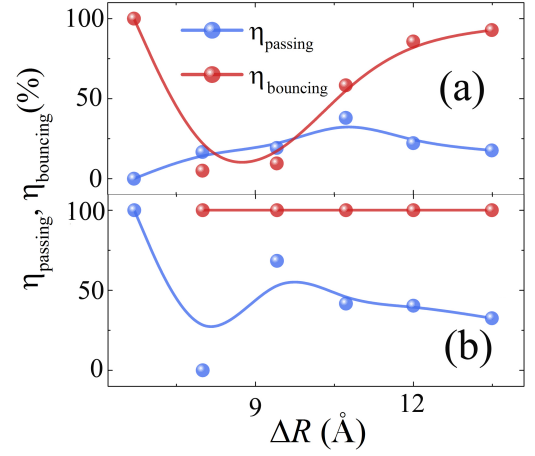


Figure 3: (a, b) Passing ratio η_{passing} and bouncing ratio η_{bouncing} as a function of diameter difference ΔR for the (a) CD defects and (b) SW defects.

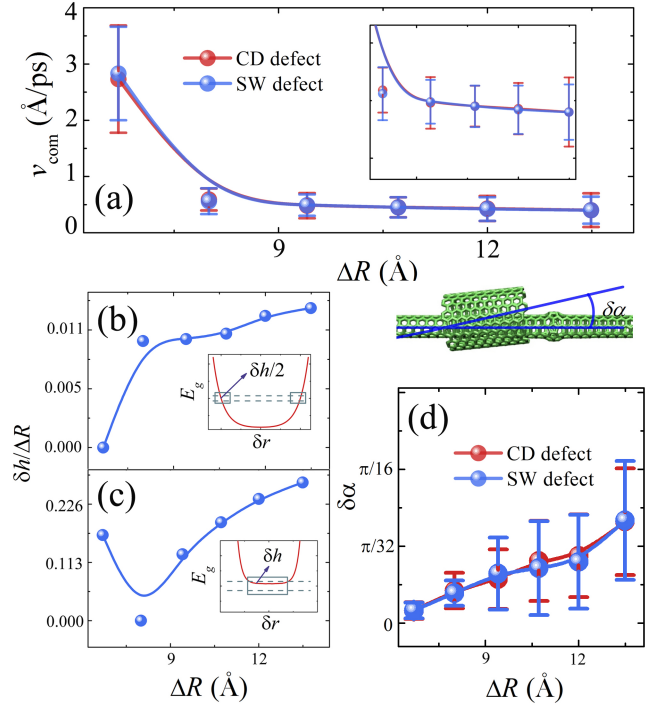


Figure 4: (a) The average velocity of the COM of the outer tube v_{COM} as functions of diameter difference ΔR . (b, c) $\delta h/\Delta R$, the configuration ratio of passing through the (b) CD defects and (c) SW defects by only considering δh . δh denotes the value span of the proper δr in which $E_g < E_k$, $E_g > 0$ and $-E_g > -E_k$, $E_g < 0$. (d) The average value of the deviation angle $\delta\alpha$ as a function of ΔR .

define a bouncing ratio to measure how often the outer tube bounces back in its failure of passing through as:

$$\eta_{\text{bouncing}} = \frac{N_{\text{bouncing}}}{N_{\text{bouncing}} + N_{\text{trapping}}} \quad (3)$$

In Fig. 3(a) and (b) we show η_{passing} varying with the diam-

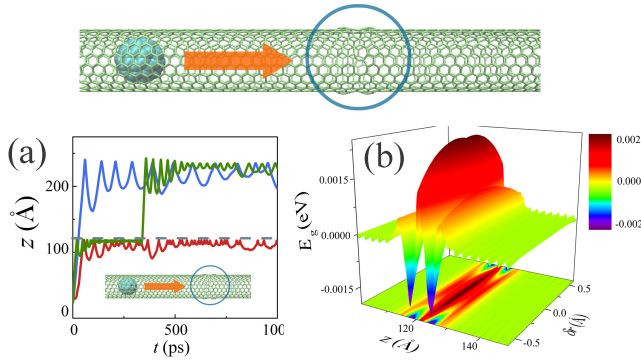


Figure 5: (a, b) Axial coordinates of a C_{60} particle and its associated van de Waals energy change E_g around the SW defects.

eter difference ΔR between the two tubes. Considering the possibility that both CD and SW defects simultaneously exist, we suggest that a proper diameter difference (neither too small nor too large) is necessary to obtain the optimal passing ratio. Figure. 3 also shows $\eta_{bouncing}$ varies with ΔR . For the CD defects, $\eta_{bouncing}$ increases with ΔR , which means the failure of passing through is more due to the potential barriers when enlarging the diameter difference. For the SW defects, $\eta_{bouncing}$ is always 100% since only potential barriers are observed in the associated E_g distribution.

Now we intend to understand the trend of the passing ratio by investigating the possible configurations of the DWNTs. Fig. 4(a) shows the average velocity of COM (v_{COM}) of the outer tube decreases with ΔR , and consequently the kinetic energy $E_k = \frac{1}{2}mv_{COM}^2$ also decrease with ΔR . The deviation distance δr varies from 0 to ΔR and only a proper δr enables the outer tube to pass through the defects, in which the kinetic energy is larger than the potential barriers ($E_g < E_k$, $E_g > 0$) and potential wells ($-E_g > -E_k$, $E_g < 0$). We denote δh as the value span of the proper δr which fulfills those requirements. Therefore, the configuration ratio of passing through can be estimated by $\delta h/\Delta R$. Fig. 4(b) and (c) show $\delta h/\Delta R$ takes a quite similar trend as the passing ratio in Fig. 3, which explains the increase of $\eta_{passing}$ with ΔR . However, after reaching the maximum value, $\eta_{passing}$ decreases with ΔR . To explain it, we propose that the contribution of $\delta\alpha$ cannot be totally neglected in outer tube with large diameter, which may result in the decrease of $\eta_{passing}$. In Figure. 4(d) we show the average value of indeed increase with in the DWNTs.

Technically speaking, the mass transportation subject could be objects inside the inner tube[11, 15, 34–36]. Fig. 5(a) shows the mass transportation of a fullerene (C_{60}) encapsulated in a (10, 10) CNT would be impeded by the defects with similar kinetic behaviors as the nanotube nanomotor in Fig. 1. It also shows that the C_{60} particle is still able to pass through the defects after a relative long time. Fig. 5(b) illustrates the distribution with associated potential barriers/wells. Adjusting to a proper configuration enables the C_{60} particle escape the defects.

CONCLUSION

In summary, we performed MD simulations on DWNTs to study the impact of defects upon the mass transportation in a nanotube nanomotor. The present simulation results have demonstrated that defects may considerably impede the thermophoretic mass transportation by the associated potential barriers and potential wells. It provides a possible picture to understand the low transportation velocity in experiments at microscopic level. Considering the impact of defects in fabricated nanotubes, we propose that a proper choose of diameter difference is essential to achieve the optimal robustness against defects. Our results will lead to improved designs and applications of nanotube nanomotors in nanoengineering.

This work was supported by National Natural Science Foundation of China (No. 21273268, 10925525, 11204341, 11290164), and Shanghai Committee of Science and Technology under Grant No. 11DZ1500400. The authors thank the High Performance Computing and Data Center, Shanghai Advanced Research Institute, Chinese Academy of Sciences.

* Electronic address: chenjige@sinap.ac.cn

- [01] Dworkin, J.; Losick, R. Proc. Natl. Acad. Sci. U.S.A. 2002, 99, 14089–14094.
- [02] Roostalu, J.; Hentrich, C.; Bieling, P.; Telley, I. A.; Schiebel, E.; Surrey, T. Science 2011, 332, 94–99.
- [03] Wickham, S. F. J.; Bath, J.; Katsuda, Y.; Endo, M.; Hidaka, K.; Sugiyama, H.; Turberfield, A. J. Nature Nanotech. 2012, 7, 169–173.
- [04] Fennimore, A. M.; Yuzvinsky, T. D.; Han, W.-Q.; Fuhrer, M. S.; Cummings, J.; Zettl, A. Nature 2003, 424, 408.
- [05] Regan, B. C.; Aloni, S.; Ritchie, R. O.; Dahmen, U.; Zettl, A. Nature 2004, 428, 924.
- [06] Regan, B. C.; Aloni, S.; Jensen, K.; Ritchie, R. O.; Zettl, A. Nano Lett. 2005, 5, 1730.
- [07] Yuzvinsky, T. D.; Fennimore, A. M.; Kis, A.; Zettl, A. Nanotechnology 2006, 17, 434.
- [08] Schoen, P. A. E.; Walther, J. H.; Arcidiacono, S.; Poulidakos, D.; Koumoutsakos, P. Nano Lett. 2006, 6, 1910–1917.
- [09] Barreiro, A.; Rurali, R.; Hernaández, Moser, J.; Pichler, T.; Forró, L.; Bachtold, A. Science 2008, 320, 775–778.
- [10] SomadaZambrano, H.; Hirahara, K.; Akita, S.; Nkayama, Y. Nano Lett. 2009, 9, 62–65.
- [11] Zambrano, H. A.; Walther, J. H.; Koumoutsakos, P.; Sbalzarini, I. F. Nano Lett. 2009, 9, 66–71.
- [12] Zhao, J.; Huang, J.-Q.; Wei, F.; Zhu, J. Nano Lett. 2010, 10, 4309–4315.
- [13] Holt, J. K.; Park, H. G.; Wang, Y.; Stadermann, M.; Artyukhin, A. B.; Grigoropoulos, C. P.; Noy, A.; Olgica, Science 2006, 312, 1034.
- [14] Joseph, S.; Aluru, N. R. Phys. Rev. Lett. 2008, 101, 064502.
- [15] Hou, Q.-W.; Cao, B.-Y.; Guo, Z.-Y. Nanotechnology 2009, 20, 495503.
- [16] Zambrano, H. A.; Walther, J. H.; Jaffe, R. L. J. Chem. Phys. 2009, 131, 241104.
- [17] Shenai, P. M.; Xu, Z.; Zhao, Y. Nanotechnology 2011, 22, 485702.

- [18] Savin, A. V.; Kivshar, Y. S. *Sci. Rep.* 2012, 2, 1012.
- [19] Santamaria-Holek, I.; Reguera, D.; Rubi, J. M. *J. Phys. Chem. C* 2013, 117, 3109–3113.
- [20] Cheh, J.; Gao, Y.; Wang, C.; Zhao, H.; Fang, H. *J. Stat. Mech.* 2013, P06009.
- [21] Kral, P.; Wang, B. *Chem. Rev.* 2013, 113, 3372–3390.
- [22] Ishigami, M.; Choi, H. J.; Aloni, S.; Louie, S. G.; Cohen, M. L.; Zettl, A. *Phys. Rev. Lett.* 2004, 93, 196803.
- [23] Sternberg, M.; Curtiss, L. A.; Gruen, D. M.; Kedziora, G.; Horner, D. A.; Redfern, P. C.; Zapol, P. *Phys. Rev. Lett.* 2006, 96, 075506.
- [24] Horner, D. A.; Redfern, P. C.; Sternberg, M.; Zapol, P.; Curtiss, L. A. *Chem. Phys. Lett.* 2007, 450, 71–75.
- [25] Wang, Q.; Ng, M.-F.; Yang, S.-W.; Yang, Y.; Chen, Y. *ACS Nano* 2010, 4, 939–946.
- [26] Stone, A. J.; Wales, D. J. *Chem. Phys. Lett.* 1986, 128, 501.
- [27] Lu, Q.; Bhattacharya, B. *Nanotechnology* 2005, 16, 555–566.
- [28] Kotakoski, J.; Meyer, J. C.; Kurasch, S.; Santos-Cottin, D.; Kaiser, U.; Krasheninnikov, A. V. *Phys. Rev. B* 2011, 83, 245420.
- [29] Contreras, M. L.; Ávila, D.; Alvarez, J.; Rozas, R. *J. Mol. Graph. Model.* 2012, 38, 389.
- [30] Allinger, N. L.; Yuh, Y. H.; Lii, J. B. *J. Am. Chem. Soc.* 1989, 111, 8551–8566.
- [31] Plimpton, S. J. *Comput. Phys* 1995, 117, 1–19.
- [32] Brenner, D.W.; Shenderova, O. A.; Harrison, J. A.; Stuart, S. J.; Ni, B.; Sinnott, S. B. *J. Phys.: Condens. Matter* 2002, 14, 783–802.
- [33] Jund, P.; Jullien, R. *Phys. Rev. B* 1999, 59, 13707–13711.
- [34] Abou-Hamad, E.; Kim, Y.; Wagberg, T.; Boesch, D.; Aloni, S.; Zettl, A.; Rubio, A.; Luzzi, D. E.; Goze-Bac, C. *ACS Nano* 2009, 3, 3878.
- [35] Skoulidas, A. I.; Ackerman, D. M.; Johnson, J. K.; Sholl, D. S. *Phys. Rev. Lett.* 2002, 89, 185901.
- [36] Shiomi, J.; Maruyama, S. *Nanotechnology* 2009, 20, 055708.